Pergamon

Int. J. Heat Mass Transfer. Vol. 38, No. 6, pp. 1043–1051, 1995

0017-9310/95 $9.50+0.00

0017-9310(94)00219-3

Prandtl number effect on offset fin heat exchanger performance: predictive model for heat transfer and pressure drop

SEN HU and KEITH E. HEROLD†

Center for Environmental Energy Engineering, University of Maryland, College Park, MD 20742, U.S.A.

(*Received* 6 *August* 1993 *and in final form* 7 *July* 1994)

Abstract—Laminar models are described which predict heat transfer and pressure drop performance of liquid-cooled offset fin cold plates. These models are developed based on a surface contribution analysis of energy and momentum balances in a unit cell of the offset fin geometry. The Prandtl number was found to have a significant influence on offset fin heat transfer. The Prandtl number effects on heat transfer are categorized into two perspectives: fin perspective and array perspective. The fin perspective Prandtl number effects explain the dependence of the periodic fully developed Nusselt number on Prandtl number. The array perspective is analogous to the thermal entry length perspective in duct flow. Array perspective Prandtl number effects yield higher Nusselt numbers in the entrance region of the offset fin array. The models predict liquid-cooled experimental data within ±20%, as compared with heat transfer and pressure drop data for Prandtl number ranging from 0.7 to 150 and Reynolds number from 10 to 2000.

INTRODUCTION AND BACKGROUND

The offset fin geometry yields a high surface compactness and good overall heat transfer performance. The present paper describes an investigation of liquid cooled offset fin heat exchangers. Although liquid cooling in such configurations has been used for many years in aerospace applications, very little data are available in the literature on this subject.

Much data are available, however, on the subject of air cooled offset fin heat exchangers. Manglik and Bergles [1] performed a comprehensive review of the state-of-knowledge of offset fin heat exchangers. It is relevant to note that no liquid-cooled studies are mentioned in that review. Joshi and Webb [2] used a surface contribution model to simulate the heat transfer and friction in the offset fin heat exchanger. The model in the present paper is based on a similar approach.

The liquid coolants of interest in the present study include water and a light synthetic oil called PAO (polyalphaolefin). The Prandtl number for these liquids ranges from 3 to 150 over the temperature range of interest (10–60°C). In the present study, the fin geometry and Prandtl number effects on heat transfer and pressure drop in offset fin arrays were studied. As a part of the effort, models of the heat transfer and pressure drop effects in laminar flow were constructed and tested against experimental data. The models, based on the surface contribution approach, form the focus of this paper.

† Author to whom correspondence should be addressed.

SURFACE CONTRIBUTION APPROACH

The geometry of the symmetric offset fin configuration considered in this study is shown in Fig. 1. The surface contribution approach used to predict heat transfer and pressure drop of these structures is similar to the approach of Joshi and Webb [2]. The model is based on the unit cell *a–b–c–d*, defined in Fig. 1(b). Four fin geometry parameters define the fin array: fin thickness (t), fin length (l), fin transverse spacing (s), and fin height (h). The surfaces in the unit cell which contribute to both the heat transfer and the pressure drop include (1) the fin sides, (2) the fin ends, and (3) the top and bottom plates. For the fin geometry, the hydraulic diameter, D_h, is defined as [3]

$$D_h = \frac{2shl}{sl+hl+th}. \quad (1)$$

Boundary layer development in an offset fin cold plate can be viewed from two distinct perspectives: (1) boundary layer development at the entrance to the fin array, which is analogous to the entrance effects in a straight duct; (2) boundary layer development on each fin, which is unique to the offset fin geometry. Both of these effects are significant in predicting heat transfer. In later discussions, boundary layer development at the entrance to the fin array is also referred to as the *array perspective* and boundary layer development on each fin is called the *fin perspective*.

For the cold plates considered in the present study, the fin array dominates the pressure drop in the system. Thus, the fin array acts as an automatic flow distributor, giving approximately equal flow to all

NOMENCLATURE

A total heat transfer area in a unit cell, $4(lh+th+ls)$
A_B leading or trailing edge area, $2th$
A_c front area of unit cell, sh
A_f frontal area of a unit cell, $h(s+t)$
A_{fin} fin area in a unit cell
A_P fin side area, $4lh$
A_T top or bottom area, $2ls$
C_D form drag coefficient
D_h hydraulic diameter of offset fin
D_h^r hydraulic diameter of rectangular duct, $(2sh)/(s+h)$
f average Fanning friction factor in offset fin
f_E average Fanning friction factor on top and bottom surfaces
f_P average Fanning friction factor on fin side
F_{unit} total friction force in a unit cell
F_D form drag force in a unit cell, $1/2\rho v^2(2th)C_D$
F_E friction force on top and bottom surfaces in a unit cell, $4ls\tau_E$
F_p friction force on fin sides in a unit cell, $4lh\tau_P$
F_α modification factor of aspect ratio
Gz Graetz number of rectangular duct
h fin height
h_0 average heat transfer coefficient of a unit cell
h_B heat transfer coefficient on downstream fin end
h_E heat transfer coefficient on top and bottom surfaces
h_F heat transfer coefficient on upstream fin end
h_P heat transfer coefficient on fin sides
j Colburn factor, $Nu_0/(Re\ Pr^{1/3})$
k thermal conductivity of fluid
k_A thermal conductivity of the cold plate
l fin length
L fin array length
L' length of a unit cell, $2l$
Nu_0 average Nusselt number in a unit cell, h_0D_h/k
$Nu_{x,E}$ Nusselt number on top and bottom surfaces, $h_ED_h^r/k$
$Nu_{x,F}$ Nusselt number of fin side in periodic fully developed thermal field
$Nu_{x,P}$ average Nusselt number of fin side in a unit cell at position x
Nu_x^m local Nusselt number of fin surface in entry region, modified from rectangular duct
Nu_F^r fully developed Nusselt number in a rectangular duct
$Nu_{F,0.5}^r$ fully developed Nusselt number in a rectangular duct with aspect ratio of 0.5
ΔP pressure drop across a unit cell
Pr Prandtl number of fluid
Q_{unit} total heat transferred in a unit cell
Q_B heat transferred on the leading and trailing ends of fins in a unit cell, $A_B\eta_B(h_B+h_f)(T_s-T_f)$
Q_E heat transferred on top and bottom surfaces in a unit cell, $(A_E\eta_Eh_E+A_Eh_E)(T_s-T_f)$
Q_P heat transferred on fin sides in a unit cell, $A_P\eta_Ph_P(T_s-T_f)$
Re^r Reynolds number of rectangular duct, uD_h^r/v
Re Reynolds number based on offset fin, uD_h/v
s spacing between adjacent fins
t fin thickness
T' local temperature in cross section
T_f average fluid temperature in a unit cell
T_s average surface temperature in a unit cell
u average fluid velocity in the area sh
u' local velocity in cross section
v average fluid velocity in the area $(s-t)h$
x distance from the beginning of a fin array
x^r distance from the beginning of a rectangular duct
x_F^+ dimensionless hydraulic fin length
x_e dimensionless hydraulic entrance length of fin array, $x/(D_h^r\,Re^r)$
x^* dimensionless thermal entry length for offset fin, $x/(D_h^r\,Re^r\,Pr)$
x_F^* dimensionless thermal fin length
x^{r*} dimensionless thermal developing length for rectangular duct, $x^r/(D_h^r\,Re^r\,Pr)$
X_{r1} reduction factor of thermal boundary developing length on fins
X_{r2} reduction factor of thermal field developing length on fin array.

Greek symbols

α aspect ratio, s/h
δ t/l
γ t/s
ρ density of fluid
ν kinematic viscosity of fluid
η overall surface efficiency, $1-(1-\eta_P)A_{fin}/A$
η_E fin efficiency of top and bottom surfaces
η_F fin efficiency of front and end surfaces of a fin
η_P fin efficiency of fin sides
θ dimensionless temperature, $(T'-T_s)/(T_f-T_s)$
τ_E shear stress on top and bottom surfaces, $1/2\rho u^2f_E$
τ_P shear stress on fin side surface, $1/2\rho u^2f_P$.

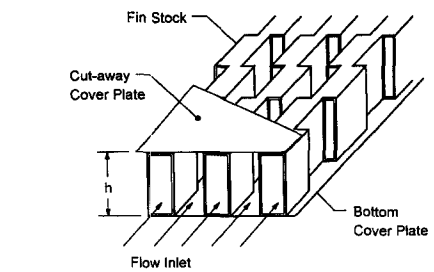

a. Perspective View

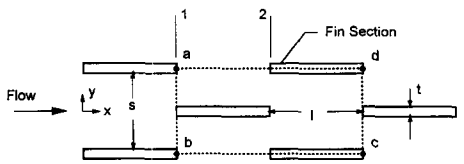

b. Cross Section View at Half Fin Height

Fig. 1. Offset fin geometry.

sections of the fin array. For more complex cold plate geometries, uneven flow distribution may contribute to more complex heat transfer characteristics. In the present study, a uniform flow distribution was assumed such that all unit cells in a row transverse to the flow are assumed to have the same characteristics. The pressure drop and heat transfer models in the study are based on laminar flow.

Pressure drop model

The model presented here predicts Fanning friction factor based on the analysis of one unit cell, *a–b–c–d*, shown in Fig. 1(b). The flow in the fin array can be analyzed similar to the flow in a rectangular duct. The Graetz number is defined to reflect the hydraulic developing length as

$$Gz = \frac{D_h^r Re^r}{x} \tag{2}$$

where x is the distance from the beginning of the fin array. From the offset fin studies of Sparrow *et al.* [4] and Kelkar and Patankar [5], it was found that, when $1/Gz > 0.005$, the flow has effectively reached a periodic hydrodynamic fully developed condition. In the current research, Reynolds numbers in the range of 10–2000 were considered and, for the fin geometries of interest, D_h^r is approximately 0.002 m. Thus, compared to the length of a typical cold plate fin array (0.3 m), the hydraulic entrance length, x_e, is so small as to be negligible. Thus, from the array perspective, the flow is treated as hydrodynamic periodic fully developed flow.

A force balance for a unit cell takes the form

$$F_{unit} = \Delta P A_f = F_P + F_E + F_D \tag{3}$$

where A_f equals $(s+t)h$. Expanding the forces in terms of shear stresses and drag coefficients yields

$$\Delta P A_f = 4lh\tau_P + 4ls\tau_E + 1/2\rho v^2(2th)C_D. \tag{4}$$

The average Fanning friction factor in the unit cell is defined such that

$$\Delta P = \frac{1}{2}\rho u^2(4f)\frac{2l}{D_h}. \tag{5}$$

Equations (4) and (5) can be combined, along with definitions of the friction factors on the various surfaces, to yield

$$f = \frac{1}{(1+\alpha+\delta)(1+\gamma)}\left(f_P + \alpha f_E + C_D\frac{t}{2l}\left(\frac{v}{u}\right)^2\right) \tag{6}$$

where δ equals t/l and γ equals t/s. Thus, the average friction factor of the offset fin array, f, can be predicted if f_P, f_E and C_D are known.

Sparrow and Liu [6] studied the friction factor of an offset fin array with zero aspect ratio so that they did not consider the influence from the top and bottom surfaces. In actual applications, the top and bottom surfaces do influence the pressure drop on the fin sides. The current model uses a rectangular duct model [7], which includes the effect from the top and bottom surfaces. In the model, the velocity is assumed uniform at the beginning of each fin. The hydraulic dimensionless fin length is defined as

$$x_F^+ = \frac{l}{D_h^r Re^r}. \tag{7}$$

From the results of Curr *et al.* [7], the friction coefficient for the fin sides has the form

$$f_P Re^r = f(x_F^+, \alpha). \tag{8}$$

The Curr data are reproduced by regression equations, in the form of equation (8) [8].

Because there are no boundary interruptions on the top and bottom surfaces, the friction factor of these surfaces is assumed to be the same as the friction factor for fully developed flow in a rectangular duct. The current model utilizes the friction factor results from Shah [9], which take the form

$$f_E Re^r = f(\alpha). \tag{9}$$

Form drag is caused by fluid flowing over finite-thickness fins. The fin drag coefficient was studied by Joshi and Webb [2], who performed pressure drop tests on offset fin arrays with water. They used a burr-free fin geometry with aspect ratio from 0.112 to 0.246. From their experimental results, they found that a constant drag coefficient C_D of 0.8 fitted the data. In the current study, a constant drag coefficient of 1.0 is used to fit our experimental data. One reason that the C_D used in the present work is larger than that of Joshi and Webb [2] is that there are burrs existing on the fins in our experimental components due to the manufacturing process. The model presented in this work

has been validated against seven actual cold plates, including the effects of burrs.

By equations (6)–(9), the average friction factor in a unit cell can be found. When the Reynolds number is low, the pressure drop is dominated by skin friction effects. At higher Reynolds number, form drag gains more significance. For example, for plate 3, the form drag component is approx. 10% of the skin friction component for a Reynolds number of 300.

Heat transfer model

Following the surface contribution approach, the average heat transfer coefficient in a unit cell is calculated by considering the heat transfer contribution from each of the surfaces. The surface contributions of heat transfer in the unit cell can be written as

$$Q_{\text{unit}} = Q_{\text{P}} + Q_{\text{B}} + Q_{\text{E}} = A\eta h_0 (T_{\text{s}} - T_{\text{f}}). \quad (10)$$

By representing each of the heat transfer rates in terms of a heat transfer coefficient, equation (10) becomes

$$A\eta h_0 = A_{\text{P}}\eta_{\text{P}} h_{\text{P}} + A_{\text{B}}\eta_{\text{B}}(h_{\text{B}} + h_{\text{F}}) + A_{\text{E}}\eta_{\text{E}} h_{\text{E}} + A_{\text{E}} h_{\text{E}}. \quad (11)$$

In equation (11), η represents the fin efficiency of the various surfaces. Since the bottom surface is heated, the fin efficiency of the bottom surface is assigned a value of 1.0. In the current model, it is assumed for simplicity that $\eta_{\text{P}} = \eta_{\text{B}} = \eta_{\text{E}}$. A one-dimensional fin model is used to compute the fin efficiency. For the liquid coolants used in the present study, fin efficiency values range from 0.6 to 0.9, as compared to values for air for the same geometry, which are very close to 1.0. The overall surface efficiency in the unit cell, η, has the form

$$\eta = 1 - (1 - \eta_{\text{P}}) A_{\text{fin}}/A. \quad (12)$$

Using equations (11) and (12), equation (10) can be transformed as follows, assuming $h_{\text{P}} = h_{\text{B}} = h_{\text{F}}$:

$$\eta h_0 = \frac{1+\delta}{1+\delta+\alpha}\eta_{\text{P}} h_{\text{P}} + \frac{\eta_{\text{P}}+1}{1+\delta+\alpha}\frac{\alpha}{2} h_{\text{E}}. \quad (13)$$

Multiplying equation (13) by D_{h}/k yields

$$\eta Nu_0 = \frac{1+\alpha}{1+\alpha+\delta}\left(\frac{1+\delta}{1+\alpha+\delta}\eta_{\text{P}} Nu_{x,\text{p}} + \frac{\eta_{\text{P}}+1}{1+\alpha+\delta}\frac{\alpha}{2} Nu_{x,\text{E}}\right) \quad (14)$$

where k is the thermal conductivity of the fluid, Nu_0 is the Nusselt number averaged over a unit cell, $Nu_{x,\text{P}}$ is the Nusselt number averaged over the fin sides in a unit cell, and $Nu_{x,\text{E}}$ is the Nusselt number averaged over the top and bottom surfaces in a unit cell. It is noted that all of these Nusselt numbers are local values in the sense that their values depend on the relative position within the fin array. The leading factor on the right hand side of equation (14) comes from the different definitions of hydraulic diameter used in $Nu_{x,\text{P}}$, $Nu_{x,\text{E}}$ and Nu_0.

To model the Nusselt number in the offset fin array, including entrance effects (array perspective), the following relationship was assumed between the offset fin array and a rectangular duct:

$$\frac{Nu_{x,\text{P}}}{Nu_{\text{F}}} = \frac{Nu_x^{\text{m}}}{Nu_{\text{F}}^{\text{r}}}. \quad (15)$$

This implies that the shape of Nusselt number profile in the entrance region is the same for both geometries. In equation (15), Nu_{F} is the Nusselt number of the fin sides (averaged over a unit cell) in the periodic fully developed section. Also, Nu_x^{m} is the local Nusselt number for thermally developing flow in a rectangular duct, which is discussed in the next section. The Nusselt number for fully developed flow in a rectangular duct, Nu_{F}^{r} [9], has the form

$$Nu_{\text{F}}^{\text{r}} = Nu_{\text{F},0.5}^{\text{r}} F_\alpha \quad (16)$$

where $Nu_{\text{F},0.5}^{\text{r}}$ is the fully developed Nusselt number in a rectangular duct with $\alpha = 0.5$, and F_α is a modification factor for the aspect ratio.

The top and bottom surfaces were modeled as if they do not experience significant periodic flow disturbances. Thus, thermal field development on the top and bottom surfaces is modeled assuming the same trend as that of a rectangular duct. The Nusselt number on the top and bottom surfaces is expressed as

$$Nu_{x,\text{E}} = Nu_x^{\text{m}}. \quad (17)$$

Once the Nusselt number on each surface is known, the average Nusselt number of a unit cell, Nu_0, can be obtained from equation (14). The heat transfer on each surface is influenced by Prandtl number. A key aspect of the present work is to investigate the effect of Prandtl number on offset fin performance.

PRANDTL NUMBER EFFECTS ON OFFSET FIN PERFORMANCE

Normally, when a fluid flows into a continuous duct, there is a developing region near the entrance of the duct, where a higher heat transfer coefficient is attained than that of the fully developed flow. The energy transfers in the entrance region are similar to boundary layer development on a plate. The transition to a fully developed condition occurs after the boundary layers forming on the walls meet in the center of the duct and the velocity and dimensionless temperature profiles become invariant in the flow direction. A fully developed velocity profile transfers less heat from a duct wall due to the convective influence of the velocity profile on the temperature profile. A fully developed temperature profile transfers less heat from a duct wall because the gradient of the temperature at the wall is reduced due to the adiabatic centerline boundary condition. The Prandtl number has a strong influence on developing heat transfer in a rectangular duct. Fluids with a large Prandtl number have longer thermal development sections. At the

same Reynolds number, the flow with higher Prandtl number has a larger Nusselt number in the entrance region. However, for laminar flow in a rectangular duct, the Prandtl number has no effect on the heat transfer in the thermally fully-developed section. Similar considerations apply to the boundary layer development on each offset fin.

Prandtl number effects from the fin perspective

For the offset fin configuration, the thermal boundary layer development on each fin has a significant effect on the heat transfer performance. An analytical investigation of developing heat transfer at the fin level was performed by Kays [10]. Later Sparrow *et al.* [4], Sparrow and Liu [6] and Kelkar and Patankar [5] developed detailed numerical models on the fin level. In all these efforts, the working fluid is air with a Prandtl number of 0.7.

Based on the assumption that the flow through fins in the offset array is similar to the flow in a rectangular duct, the rectangular duct is used as a model to predict fin performance in the current work. Montgomery and Wilbulswas [11] developed a numerical model of heat transfer in the thermal developing section of a rectangular duct with uniform surface heating. Their study demonstrated a significant Prandtl number influence on heat transfer in the simultaneously developing hydrodynamic and thermal regimes with velocity and temperature uniform at the entrance of the duct. For Prandtl number near unity, the temperature and velocity boundary layers develop at about the same rate. For fluids with a larger Prandtl number, such as water (Pr = 3–10) or polyalphaolefin (PAO) (Pr = 40–150), the velocity boundary layer is much thicker and the hydraulic entry length is much shorter than the corresponding thermal characteristics.

Heat transfer in a developing, laminar, high-Prandtl number flow in a rectangular duct, with uniform velocity and temperature profiles at the entrance was computed by Montgomery and Wilbulswas [11]. Their results are used in our model to predict the heat transfer characteristics of the offset fin configuration by viewing the flow between offset fins as developing flow in a rectangular duct.

The design concept of the offset fin geometry is to present each fin with uniform temperature and velocity fields, so that the heat transfer characteristics approximate those of the entrance region of a duct. However, in practice, the fins are closely spaced and the boundary layers which form on each fin are still present, although altered by diffusion and convection effects, when the next fin is encountered. The effect of this non-uniform boundary condition for each fin is to reduce the heat transfer from the fin, as compared to an entrance region model. However, the offset fin heat transfer is still considerably greater than that for a continuous fin of the same area.

Two-dimensional predictions of the velocity and temperature fields in an offset fin geometry with zero thickness fins are plotted in Fig. 2, based on data from Sparrow *et al.* [4]. Figure 2(a) and 2(b) shows the velocity and temperature profiles, at positions 1 and 2 in Fig. 1, in the periodic fully developed region. Figure 2(c) shows the temperature profiles, at positions 1 and 2 in Fig. 1, in the hydraulic and thermal entrance region. The influence of the upstream fins on the downstream fins is evident in the temperature and velocity traces. This influence tempers the heat transfer benefit of the offset fin geometry. However, for real fins of finite thickness, Joshi and Webb [2] and Mochizuki *et al.* [12] found that small vortices are formed after each fin at sufficiently high Reynolds number. The mixing of the fluid caused by the swirling flow reduces the temperature nonuniformity seen by the downstream fin. The average Nusselt number for the entrance region of a rectangular duct was computed by Montgomery and Wilbulswas [11]. A data regression was performed on their results to yield an equation of the form

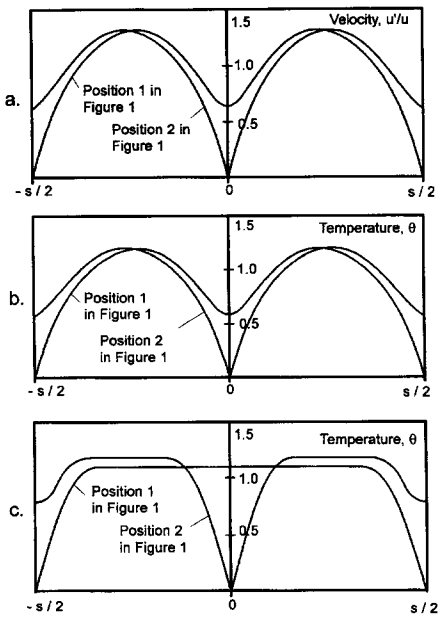

Fig. 2. Offset fin velocity and temperature profiles from [4]: (a) fully developed velocity, (b) fully developed temperature, and (c) developing temperature.

$$Nu_F = f(Pr, x^*, \alpha). \tag{18}$$

Considering the influence of the nonuniform fluid temperature and velocity at the beginning of each fin, this result was modified into the form

$$Nu_F = f(Pr, x^*_F, \alpha, X_{r1}) \tag{19}$$

The factor X_{r1} is introduced to reduce the effective development length along a fin. This factor was determined from our experiments to have the form

$$X_{r1} = 3.63 + 6.67 \log_{10}\left(Pr\left(\frac{D_h}{l}\right)^{0.15}\right). \tag{20}$$

It is well known that, for a high Prandtl number fluid, the thermal boundary layer develops much slower than the hydrodynamic boundary layer, because the thermal diffusivity is relatively low compared to the momentum diffusivity. In the offset fin geometry, a large Prandtl number causes larger temperature nonuniformities at the beginning of each row of fins. The fin geometry ratio D_h/l also influences the temperature nonuniformity. Shorter fin length and larger hydraulic diameter tend to cause larger temperature nonuniformity. In equation (20), it is seen that X_{r1} increases with both Prandtl number and D_h/l. An increase in X_{r1} means an increase in the effective dimensionless fin length, which implies decreased average heat transfer.

In equation (19), Nu_F is the average Nusselt number on the fin sides of one unit cell. This model for Nu_F applies to the periodic fully developed flow regime. Due to the interruptions of the thermal boundary layer development on the fins, the periodic fully developed heat transfer is higher than that of fully developed flow in a comparable rectangular duct. Different from rectangular ducts, the Nusselt number for periodic fully developed heat transfer in an offset fin array is influenced by both Reynolds and Prandtl numbers. This point is returned to after discussion of entry length considerations from the array perspective.

Prandtl number effects from the array perspective

When air flows into an offset fin array with a uniform velocity profile, the flow achieves periodic fully developed velocity and temperature profiles after less than 10 fin lengths, depending on Reynolds number [4]. For a high Prandtl number fluid, however, the thermal field development occurs over a greater length. Eventually, a periodic fully developed temperature field does develop, but for high Prandtl number fluids the cold-plate characteristics are significantly impacted by entry length effects.

The heat transfer in the offset fin entrance region is simulated here analogous to entrance region heat transfer in rectangular ducts. Sparrow *et al.* [4] and Kelkar and Patankar [5] used numerical calculations to simulate the thermal entrance region in an offset fin array using air. A comparison of the thermal entry length between their work and rectangular ducts with constant wall temperature [13] shows a dramatic reduction in the developing length for the offset fin geometry (reduction by a factor of 10).

The thermal entrance length of the offset fin geometry is about 10% of that in a rectangular duct. There are two effects causing the entry length to be shorter in the fin geometry as compared to a rectangular duct. One effect is associated with the definition of the hydraulic diameter, D_h^r, where the channel width is chosen as s. From an entry length perspective, the effective channel width is more like $s/2$, since the temperature boundary layers form on all fins and meet in the middle of each channel of width $s/2$. This accounts for a factor of two difference in the entry length. Another factor which significantly reduces the thermal entry length for the offset fin geometry is the convection of energy associated with the transverse velocity component. Due to the periodic geometry of the fins in the flow direction, the velocity boundary layer formation causes the transverse velocity to fluctuate around zero. This transverse convection has a mixing effect, which increases the transfer of energy into the bulk flow and results in a shorter entry length. Both factors make the thermal entry length shorter than that of the rectangular duct. As mentioned above, all known thermal entry length calculations for the offset fin geometry are based on air. For the high Prandtl number fluids of interest in the current study, no entry length calculations were found in the literature. For the present model, it is assumed that dimensionless thermal entry length is 10% of that of a rectangular duct. This effect is represented by a reduction factor, $X_2 = 10$, in later equations.

Developing heat transfer in a rectangular duct was calculated by Montgomery and Wilbulswas [11]. These results are used in the present study, modified based on the above entry length discussion, to yield a function of the form

$$Nu_x^m = f(Pr, x^*, \alpha, X_{r2}). \quad (21)$$

The thermal field development from the array perspective affects the heat transfer on all fin surfaces, including fin sides and top and bottom surfaces. This point is returned to in the discussion section which follows.

DISCUSSION

In Fig. 3(a) and (b), the predicted Nusselt number on the fin sides is plotted vs plate length, with different Prandtl numbers at two Reynolds numbers for plate 3. Plate 3 is one of seven offset fin cold plates on which experiments were conducted [8] as a part of this study. The geometry details of plate 3 are included on Fig. 3. In Fig. 3, the abscissa is the distance from the inlet of the fin array. The ordinate is the local Nusselt number of the fin side-averaged over one unit cell. From equations (15)–(17) and (19), the Nusselt number on the fin sides is seen to be influenced by Reynolds number, Prandtl number and fin geometry. It is observed that the array perspective effects have a significant influence on the heat transfer performance when Reynolds and Prandtl numbers are large. At the entrance of the fin array, the Nusselt number is high because of the thermal field development. Along the fin array, the thermal field develops until it reaches the periodic fully developed condition. A larger Prandtl number implies a longer distance to achieve a periodic fully developed thermal field (array perspective effects). Unlike the fully developed heat transfer in a continuous duct, the periodic fully developed Nusselt

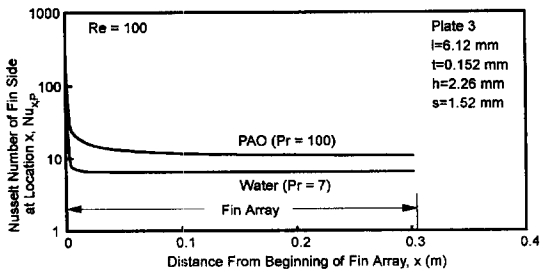

a. Results for Reynold's number of 100.

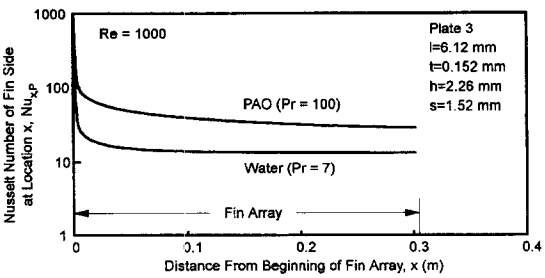

b. Results for Reynold's number of 1000.

Fig. 3. Thermal development from the array perspective.

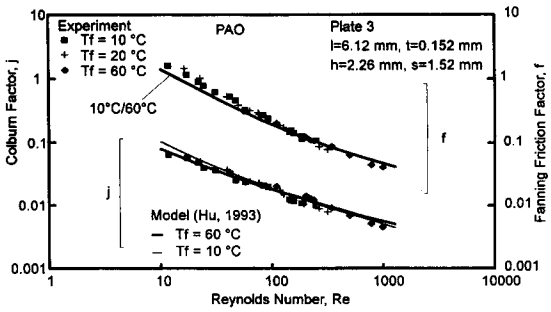

a. Results for PAO

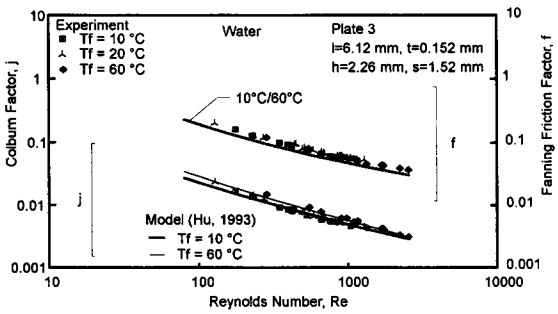

b. Results for water

Fig. 4. Effect of fluid temperature on performance of an offset fin cold plate.

number for the offset fin geometry is dependent on Prandtl number. This is because the offset fin interrupts the flow periodically, causing a thermal boundary layer to develop on each fin. Therefore due to the periodic interruptions in the fins, the heat transfer in the periodic fully developed thermal field is influenced by both Reynolds and Prandtl numbers. The flow with larger Prandtl number has a longer thermal developing region on each fin, which achieves a higher average heat transfer over the fin (fin perspective effects).

Comparing Fig. 3(a) and (b), it can be seen that a larger Reynolds number increases Nusselt number from both the fin and the array perspectives. From the array perspective, an increase in Reynolds number extends the thermal entry length. From the fin perspective, a larger Reynolds number extends the high Nusselt number region on each fin by reducing the boundary layer thickness, causing a higher periodic fully developed Nusselt number. Figure 3(a) displays a case with relatively small Reynolds and Prandtl (water) numbers and the thermal field development from the array perspective has a relatively small effect on overall heat transfer. In contrast, Fig. 3(b) displays a case with large Reynolds and Prandtl numbers, which is affected by thermal development from both the array and fin perspectives. These characteristics are integrated into the surface contribution model to predict the overall heat transfer.

A comparison of model results with experimental data [14] is made in Fig. 4(a) and (b), where Colburn factor and friction factor are plotted vs Reynolds number at different fluid temperatures. In Fig. 4(a) and (b), the experimental data for j appears to increase slightly with fluid temperature. This effect can be explained in terms of Prandtl number. In Fig. 4(a), where PAO is used as the coolant, the Prandtl number ranges from 150 to 40 as temperature ranges from 10 to 60°C. The curves representing the model results exhibit significant Prandtl number effects, as shown by the intersection of the j curves for 10 and 60°C. The low temperature case has a high Prandtl number and consequently a higher overall j, at high Reynolds number, because of entry length effects. In Figure 4(b) where water is used as the coolant, the Prandtl number ranges from 10 to 3 as temperature ranges from 10 to 60°C. Because of the smaller Prandtl number compared to PAO, no cross-over is observed in the j curves. The model results of the Colburn factor at different fluid temperatures compare well with test data. For plate 3, the model predicts 94% of the Colburn factor data within $\pm 20\%$, and 90% of the Fanning friction factor data within $\pm 20\%$. The comparison of the model against experimental data for the other six tested plates gives similar results.

Model predictions of Colburn factor and friction factor are plotted in Fig. 5 vs Reynolds number for air, water and PAO. A comparison is made against air correlations from Wieting [15] and Joshi and Webb [2] (corrected to match the hydraulic diameter used in the current research). Prandtl number has a significant effect on the Colburn factor, as seen in Fig. 5. Air, with Prandtl number of 0.7, has the smallest thermal entry length effect (array perspective Prandtl number effect). At low Reynolds number the curves for the higher Prandtl number fluids have a similar shape j curve to that of air. This is because the array per-

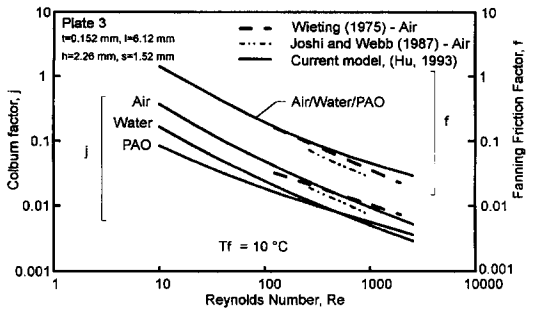

Fig. 5. Comparison of current model with other models.

spective effect is small at low Reynolds number. As the Reynolds number becomes larger, the j curve for high Prandtl number changes slope. This is because the array perspective effect becomes larger, which increases the overall heat transfer in the fin array. Since PAO has a higher Prandtl number than water, the effects are most pronounced for PAO.

Wieting [15] and Joshi and Webb [2] considered only air as coolant. Reasonable agreement was found between their results and our model, with air as the coolant, as seen in Fig. 5. It should be noted that the results of Wieting [15] and Joshi and Webb [2] were obtained from constant surface temperature boundary conditions and the current results (experiments and model) were obtained based on constant heat flux boundary condition.

The friction factor curves for different Prandtl numbers are coincident. The current model predictions of friction factor are higher than the results of Wieting [15] and Joshi and Webb [2], but these predictions match our liquid data quite closely. It is known that burrs on the fins increase form drag. The burrs are caused by the process of manufacturing the fin stock. In Kays and London [3], burr effects are shown to increase the friction factor. The fin stock used in the experiments in the present study was manufactured by standard methods which result in significant burrs. The size of burrs is documented by Hu [8]. The model put forward here is designed to represent real-world offset fin practice.

It has been suggested that air correlations could be used for liquid cooled designs [3]. In Fig. 5, it can be seen that the models of Wieting [15] and Joshi and Webb [2] overpredict the Colburn factor for liquids at a given Reynolds number. This implies that air models cannot be used for liquid applications. The difference in Colburn factor between liquid and air is approximately a factor of two. If the Wieting correlation is used for a liquid application, it will predict the temperature difference between the surface and the fluid twice as small as the actual situation.

CONCLUSION

The Prandtl number has a significant effect on the heat transfer performance of the offset fin cold plate. For large Prandtl number, thermal field development in the fin array and thermal boundary layer development on the fins are both significant. An increase in Prandtl number tends to cause an increase in the average Nusselt number of the fin array from both of these effects.

A laminar flow model is described, considering the Prandtl number, Reynolds number and fin geometry effects. The model can predict the heat transfer and pressure drop of offset fin arrays with Prandtl number from 0.7 to 150. Within a deviation of $\pm 20\%$, the model predicts 94% of Colburn factor test data and 90% of friction factor test data. Literature models for air-cooled offset fin arrays do not accurately predict liquid cooled characteristics. The models for air overpredict the Colburn factor for liquid coolants. The overprediction of Colburn factor is about 100%, which is unacceptable in typical thermal design.

Acknowledgements—The authors would like to express appreciation to Westinghouse Electric Corp. for sponsoring this work. In particular, discussions with Frank Altoz were most helpful.

REFERENCES

1. R. M. Manglik and A. E. Bergles, The thermal-hydraulic design of the rectangular offset-strip-fin compact heat exchanger. In *Compact Heat Exchangers* (Edited by R. K. Shah, A. D. Kraus and D. Metzger), pp. 123–149. Hemisphere, New York (1990).
2. H. M. Joshi and R. L. Webb, Heat transfer and friction in the offset strip-fin heat exchanger, *Int. J. Heat Mass Transfer* **30,** 69–84 (1987).
3. W. M. Kays and A. L. London, *Compact Heat Exchangers* (3rd Edn). McGraw-Hill, New York (1984).
4. E. M. Sparrow, B. R. Baliga and S. V. Patankar, Heat transfer and fluid flow analysis of interrupted-wall channels with application to heat exchangers, *J. Heat Transfer* **22,** 1613–1625 (1977).
5. K. M. Kelkar and S. V. Patankar, Numerical prediction of heat transfer and fluid flow in rectangular offset-fin arrays, *Numer. Heat Transfer A* **15,** 149–164 (1989).
6. E. M. Sparrow and C. H. Liu, Heat-transfer, pressure-drop and performance relationships for in-line staggered and continuous plate heat exchangers, *Int. J. Heat Mass Transfer* **22,** 1613–1625 (1979).
7. R. M. Curr, D. Sharma and D. G. Tatchell, Numerical predictions of some three dimensional boundary layers in ducts, *Computer Meth. Appl. Mech. Engng* **1,** 143–158 (1972).
8. S. Hu, Heat transfer and pressure drop of liquid cooled offset fin heat exchanger. PhD Dissertation, University of Maryland (1993).
9. R. K. Shah, *Laminar Flow Forced Convection in Ducts—a Source Book for Compact Heat Exchanger Analytical Data.* Academic Press, New York (1978).
10. W. M. Kays, *Compact Heat Exchangers.* AGARD Lecture Series # 57 on Heat Exchanger, AGARD-LS-57-72 (1972).
11. S. R. Montgomery and P. Wilbulswas, Laminar flow heat transfer for simultaneously developing velocity and temperature profiles in ducts of rectangular cross section, *Appl. Sci. Res.* **18,** 247–259 (1967).
12. S. Mochizuki, Y. Yagi and W. J. Yang, Flow pattern and turbulence intensity in stacks of interrupted parallel-

plate surfaces, *Expl Thermal Fluid Sci.* **1,** 51–57 (1988).
13. R. K. Shah and A. L. London, Effects of nonuniform passages on compact heat exchanger performance, *J. Engng Power* **102,** 653–659 (1980).
14. S. Hu and K. E. Herold, Prandtl number effect on offset fin heat exchanger performance: experimental results, *Int. J. Heat Mass Transfer* **38,** 1053–1061 (1995).
15. A. R. Wieting, Empirical correlations for heat transfer and flow friction characteristics of rectangular offset-fin plate-fin heat exchangers, *Trans. ASME J. Heat Transfer* **97,** 488–490 (1975).